University of Thi-Qar Journal of Science (UTJsci)
E-ISSN: 2709-0256, P-ISSN: 1991-8690, Vol. 13, No. 1, Jun. 2026

Characterization of Green Synthesized Zinc Oxide Nanoparticles from Two *Quercus* species Leaf Extracts Based on Their Phytochemical Profiles

Dilan Mohammed Azezz Saleem[1a] and Sirwa Anwar Qadir[1b*]

[1]*Departmrnt of Forestry, College of Agricultural Engineering Science, Salahaddin University, Erbil, Iraq.*
[a]E-mail: dilanakrayi92@gmail.com
[b*]Corresponding author: sirwa.qadir@su.edu.krd

Received: 23-10-2025, Revised: 07-12-2025, Accepted: 20-12-2025, Published: 01-06-2026

***Abstract*— The variation, in the secondary metabolite profile of trees is greatly affected by the climatic conditions. The main aim of the study was to compare the phytochemical profiles of *Quercus brantii* and *Quercus infectoria* leaves and evaluate their effectiveness in green synthesis of ZnO NPs. Phytochemical variation of leaves of two abundant oak species in Barzewa forest, *Q. brantii* and *Q. infectoria* leaves has been examined and the role of their aqueous leaf extract in green synthesis of zinc oxide nanoparticles has been studied. *Q. brantii* leaves was significantly higher in total phenol and flavonoid contents (10.50 and 0.267 mg/g) compared to *Q. infectoria* (8.41 and 0.026 mg/g) respectively. While, tannin content did not differ significantly between the two species. Both species' role was confirmed as reducing and stabilizing co- factors in the conversion of ZnO metal oxide to nano ZnO. UV–visible spectroscopic analysis verified successful synthesis with a specific ZnO NPs peak absorbance at 370.4 nm for *Q. brantii* and 374 nm for *Q. infectoria*. In both species a consistent peak at 399.35 cm^{-1} evidenced the presence of Zn–O stretching vibration in Fourier Transform Infrared spectroscopy (FTIR) analysis. Whereas X-Ray Diffraction spectroscope (XRD) confirmed wurtzite hexagonal structure crystals for both species. ZnO- mediated by *Q. brantii* leaves yielded a smaller crystallite size 27.55 nm compared to *Q. infectoria*, which produced ZnO NPs with 46.12 nm. Scanning electron microscopy (SEM) revealed that smaller, more homogeneous particles were generated with *Q. brantii*, with an average diameter of 46.11 nm. In comparison, larger diameter (50.01 nm) and more heterogeneous nanoparticles were generated by *Q. infectoria*. The findings of the study highlight the significant role of selecting specific species of any plant depending on their phytochemical profile for optimizing the nanomaterial synthesis-based plants.**

***Keywords*— Oak; XRD; Nanoparticle; Phenol; Flavonoids**

I. INTRODUCTION

Although the first creation of "nanotechnology" belongs to 1974, its origins back to 1959 [1]. Due to their distinctive properties, nanoparticle have become a modern, revolutionary invention, and widely used in contemporary science. It has a wide application in various life disciplines like agriculture, medicine, and industry [2]. In agriculture, they played a significant role in safeguarding crops, nutrient transport, and boosting plant growth [3]. Nanoparticles (NPs) are extremely significant due to their better physicochemical and biological characteristics compared to the bulk material. They have greater surface reactivity, because of their tiny size (1–100 nm), which makes them to have a higher ratio of surface: volume [4]. Metal oxides nanoparticle such as Zinc oxide (ZnO) nanoparticles gained a particular interest of use because of their chemical stability, broad radiation absorption, high electrochemical coupling coefficient, UV-blocking behavior, photocatalytic activity, and antimicrobial properties. These characteristics make ZnO NPs valuable in environmental remediation, agriculture, food packaging, cosmetics, and biomedical fields [5]. Synthesizing ZnO NPs via chemical and physical routes often requires higher consumption of energy, and involve toxic and harmful chemicals that threaten the environment and living organism health. In contrast, bio- methods for synthesizing ZnO NPs offers an offer eco-friend and cost-efficient alternatives [6]. Biological synthesis employs living materials such like; bacteria, fungi, and plant extracts, they were act as reducer and stabilizer agents [7]. Plant extracts, in particular, have gained wide popularity as reducing and stabilizing agents due to their rich content of phytochemicals such as tannins, flavonoids, phenolic acids, terpenoids, and alkaloids. The phytochemicals participate directly in reducing Zn^{2+} ions and stabilizing the resulting ZnO-NPs, while also influencing the nanoparticles' size, morphology, crystallinity, and stability [8]. Previous studies have demonstrated the role of different plant extracts in ZnO NP synthesis [9]. Many types of plants have been used in the manufacturing of ZnO NPs; namely, aloe vera (Izwanie et al., 2020), *Moringa oleifera* leaf extract [10], *Ocimum basilicum* [11], rosemary leaves (Noukelag et al., 2020), *Azadirachta indica* leaves (Iqbal et al., 2021), *Lycopersicon esculentum* [12], and *Cassia fistula* and Eucalyptus leaf extract [13]. But the efficiency of the extract strongly depends on the accumulated secondary metabolites in plant tissues, because they produced as a defense mechanism, that remark their degree of tolerance against biotic and abiotic stress factors in their environment [14]. Even their concentrations varied in different plant parts (leaves, roots, bark, flowers, fruits, and seeds) [15]. The environmental factors like; soil profile content, climate, elevation, and biotic life interactions regarded as the main reason for inducing such variation among the same species of genus as well as plant body parts within the species [16]. Oak tress is well known by its medicinal use due to its rich phytochemical content in their leaves and acorns [17]. Varied altitude and geospatial variations as well as the climate changes in the north of Iraq made a great diverse in the growth of the trees and their bio- chemical contents [18]. Oak trees make up to 4% of the total forest region in the area.

https://doi.org/10.32792/utq/utjsci/v13i1.1504

They are abundant in the northeast; near the Iranian border at Hurin Sheren and Turkish border at Zakho, with latitudes between 34° 40' and 37° 08' and longitudes between 42° 40' and 45° 30' [19]. In iraqi Kurdistan forests *Q. brantii, Q. libani, Q. infectoria, and Q. macranthera* are regarded as most abundant oak species [20]. The climate variables affect the presence records in distribution target species and their defense mechanisms to combat the climate changes by producing various secondary metabolites [21-22]. As the phytochemical composition of plant extracts have a crucial role on the quality of ZnO-NPs, evaluating these compounds in *Q. brantii* and *Q. infectoria* is necessary. Differences in polyphenol, flavonoid and tannins content may directly affect nanoparticle formation, stability, and functional properties. Therefore, , the aim of this study is to compare the phytochemical profiles of *Q. brantii* and *Q. infectoria* leaves and to investigate their effectiveness in the green synthesis of zinc oxide nanoparticles.

II. Material and Methods

Collection of leaf samples: Mature leaves of 30 trees of *Q. brantii* and Q. *infectoria* were gathered from Barzewa forest. The leaves were washed with tap water, then rinsed with distilled. Barzewa is a mountainous area characterized by high altitudes, with an average elevation of approximately 1,800 meters. It belongs to Soran District in Erbil province in Iraqi Kurdistan region. Its coordinates "Latitude: 36.62461° N and Longitude: 44.61258°. The cleaned leaves shed dried at room temperature (20–30 °C) temperature, and grinded slowly then sieved using 25-mesh to have a smooth powder, and finally the powder kept in tightly sealed dark glass bottles at 4 °C.

A. Phytochemical screening of Quercus app. Leaves

Preparation of leaf extract: dry powder (10 g) of each species was extracted in 100 ml ethanol for three days with regular stirring at room temperature. A guarantee of extraction process is given by repeating it three times. For obtaining the crude extracts it was filtered twice using Whatman NO.1 filter paper followed by concentrating it using rotary evaporator [23].

Total phenol content (mg/g): It was measured in the leaf extract measured in the leaf extract using the Folin–Ciocalteu reagent method [24]. Briefly, 0.125 ml of the extracts was mixed with 0.5 mL of distilled water and 0.125 mL of Folin-Cicalteau's reagent. After 6 min, 1.25 mL of 7.5% aqueous Na2CO3 solution was added. The final volume adjusted to 3 mL with distilled water and mixed vigorously and then kept at room temperature for 90 min. Finally, the absorbance of the extract was measured at 760 nm (HACH DR/4000U-USA- Spectrophotometer). The total phenolic content was expressed as mg of gallic acid per g of dry weight.

Total flavonoids content (mg/g): The leaf extract flavonoids content was determined using the aluminum chloride colorimetric method [25]. 0.5 ml of the extract was mixed with 0.5 ml of 2% aluminum chloride methanol solution. After 15 min keeping at at room temperature, the absorbance was measured at 430 nm using spectrophotometer (HACH DR/4000U-USA). The total flavonoid content was expressed as mg of rutin equivalents per grams of leaf dry weight.

Total tannin content (mg/g): Tannins were determined using the Folin- Ciocalteu colorimetric method with the standard tannic acid compound [22]. 1 ml of 10-fold diluted extracts, 5 ml of 2.5% KIO3 were mixed in a vial and vortexed for 10 seconds. The absorbance of the mixture (red color) was measured at 550 nm. Different standard concentrations of tannic acid solutions (100 to 1600 mg/ml) were used to calibrate and standard curve preparation. The final results were expressed as mg tannic acid per gram of leaf dry powder.

Data analysis: An independent t-test was based to compare the phytochemical profile; phenol, flavonoids and tannins for the thirty individual trees of the two species. The difference was statistically significant when *P*- value < 0.05. Results are presented as mean ± standard error (SE).

B. Preparation of leaf extract and synthesizing ZnO NPs:

Fifty grams of powdered leaf was added to distilled water (300 ml) in boiling water bath for 30 minutes. Kept for another 30 minutes at 60 °C to ensure successful bioactive compounds extraction. The precipitant was removed in leaf extract through a filtration process to obtain a clear filtrate and stored at 4 °C. The leaf extract (50 mL) of both species was heated gently (60 °C). An amount of 1.10 g of zinc acetate- dihydrate Zinc acetate dihydrate ($Zn(CH_3COO)_2 \cdot 2H_2O$, ≥ 99% purity, Sigma-Aldrich, USA) was added to the extract. The mixture was then constantly mixed for an hour under and the temperature was kept at 60 °C, and till turned to a brownish paste, which is a visible remark for the production of NPs. The paste was calcined at 400 °C for two hours in a muffle furnace, after cooling to room temperature, the ZnO NP powder was washed several times with distilled water and ethanol.

C. Characterization of ZnO NPs:

- Ultraviolet -visible spectroscopic analysis: The optical properties of the ZnO NPs were measured by ultraviolet- visible (UV–Vis) spectroscopy using the Kenza 240 Tx spectrophotometer (single- and double- beam capable) [26].
- Fourier Transform Infrared- spectroscopic (FTIR): (FTIR- SHIMADZU/ Japan) Spectroscopy used to identify the presence of functional groups that mediated the reduction of metal ions into nanoparticles.
- X- Ray Diffraction Spectroscopy (XRD): Crystalline phase identification determination was performed using (PANalytical X'Pert PRO X- Ray Diffractometer) The size of crystals being computed according to Debye Scherrer equation [27]:

  $$D = 0.9\lambda/\beta\cos\theta$$

  Where 0.9 is the shape factor (Scherrer constant), D is the mean of crystal size, K is shape factor, ʎ is X-Ray wavelength, β is the half of maximum width, and θ is the diffraction angle.
- Energy Dispersive X-Ray Spectroscopic (EDX): The elemental composition of the ZnO NPs were analyzed using FEI Quanta 450 Scanning Electron Microscope (SEM) equipped with a Bruker EDS (Energy- Dispersive X- Ray Spectroscopy) [28].
- Scanning Electron Microscope Analysis: The morphological characters of NPs checked using FEI Quanta 450- SEM, imaged under appropriate accelerating voltage (e.g., 10–20 keV) [29].

III. Result and Discussion

A. Phytochemical screening of Quercus app. Leaves

The phytochemical profile of *Q. brantii* and *Q. infectoria* revealed a significant variation in the phenolic and flavonoid content in their leaves. A significant and higher total phenolic content was exhibited by *Q. brantii* was (10.50 mg/g) compared to *Q. infectoria* that had 8.41 mg/g. Similarly, higher total flavonoid content was denoted by *Q. brantii* (0.267 mg/g) as compared to *Q. infectoria* that stored 0.026 mg/g of flavonoids in their leaves. In contrast, the tannin remains constant and not varied between the species (Table 1). The observed phytochemical profiles align with other researches on *Quercus* species, which are known for their rich composition of secondary metabolites of Iranian oak [30]. The significant difference in the total phenol and flavonoid contents in both species suggests a species depended variation in the biosynthesis and accumulation of such compounds, even when they were habituated Barzewa forests (relatively high altitude of this area (approximately 838 m above sea level) might be played a great role in the chemical content variations. [31-32] confirmed that higher altitudes greatly affect the flavonoid compounds, because in higher altitudes the UV radiation increased and temperatures lowered significantly, which enhances the plant to activate their antioxidant defense system in the plant body. While, [33] revealed that the concentration of the secondary metabolites mostly affected by altitude in comparison to primary metabolites, because they derivates in response to the stress factors in the environment.

Table 1: Phytochemical screening of *Quercus* spp. Leaves

Quercus spp.	Total phenols (mg/g)	Total flavonoids (mg/g)	Tannins (mg/g)
Q. brantii	10.50 ± 1.01 a	0.267 ± 0.02 a	0.06 2± 0.09 a
Q. infectoria	8.41 ± 2.01 b	0.026 ± 0.09 b	0.061±0.08 a
P-value (Sig.2-tailed)	0.007< 0.05	0.001< 0.05	0.12> 0.05

B. Characterization of ZnO NPs:

The surface plasmon resonance (SPR) reflects metal ion reduction to nanoparticle, which resulted in interacting electromagnetic waves with electron conduction band oscillation which was detected using UV–visible spectroscopy [34]. The absorption spectra (Figures 1 and 2) were confirmed the formation of ZnO- NP synthesized using *Quercus brantii* and *Quercus infectoria* extracts, respectively. Both samples exhibited absorption peak characteristics within the range of 360–380 nm, which is typical for ZnO nanoparticles due to their intrinsic band-gap absorption [35]. When *Q. brantii*-mediated the synthesis process, an observed peak was at 370.4 nm and had 0.787 absorbance value (Figure 1). Similarly, *Q. infectoria* showed a strong peak at 374 nm, but an absorbed value was at 1.46 (Figure 2). This slight difference in the absorbance value indicates higher yield of the NPs or they have smaller diameters of *Q. infectoria* compared to *Q. brantii*. A strong peak appeared in the UV region (370–374 nm), followed by a gradual decrease in absorbance as previously was proved by [36-38]. As well as the tailing phenomenon ensures that the particles are within the range of nanoscale [39]. *Quercus brantii* and *Quercus infectoria* leaf extracts are rich phytochemicals (Table 1) facilitated the conversion of Zn^{2+} ions from zinc acetate dihydrate into ZnO nanoparticles.

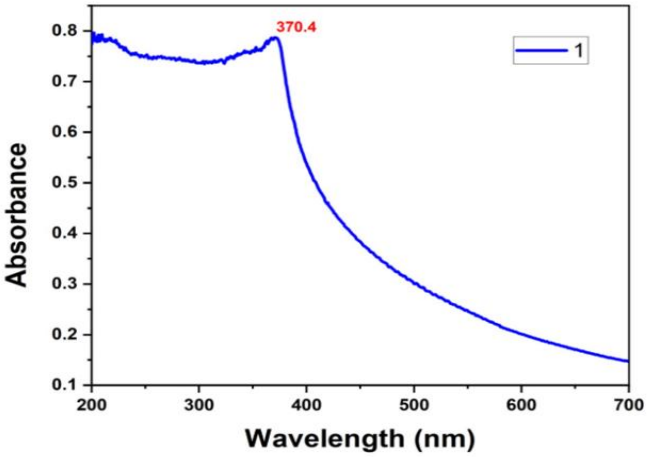

Fig. 1: UV Vis peaks of ZnO NP mediated with *Q. brantii* leaves

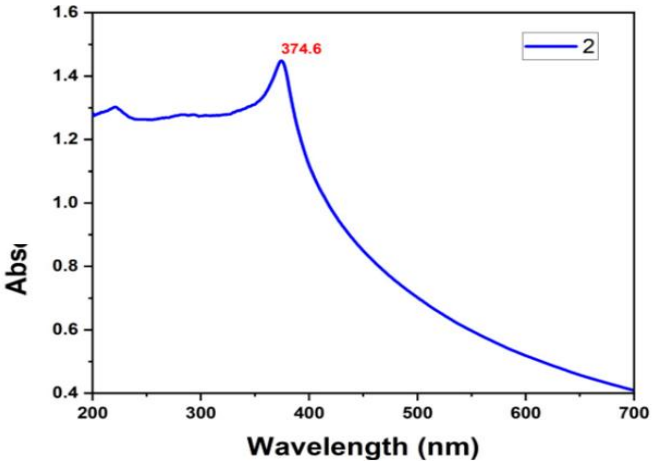

Fig. 2: UV Vis peaks of ZnO NP mediated with *Q. infectoria* leaves

The spectra obtained from FTIR for *Quercus brantii* and *infectoria* showed different peaks belongs to the functional groups in both extracts that functioned greatly in nanoparticle formation. Successful production of ZnO nanoparticles in both samples was confirmed by the observation of a consistent peak for both spectra at 399.35 cm^{-1}, that belongs to stretching vibrations of Zinc- oxygen bond (Zn–O). Despite having the lowest intensity (10.00) in both instances (Figures 3 and 4), this peak had the biggest area, suggesting a wide absorption range characteristic of ZnO nanoparticles, which are distinguished by their heterogeneous nature and large surface area [40-41]. The FTIR spectrum of *Quercus brantii* showed notable peaks at 867.65 cm^{-1}, 1052.96 cm^{-1}, 1414.96 cm^{-1}, and 1483.91 cm^{-1} (Figure 3). These peaks were attributed to C–H bending in aromatic rings (867.65 cm^{-1}), C–O stretching (1052.96 cm^{-1}), and vibrations of C=C in aromatic rings (1414.96 and 1483.91 cm^{-1}). These peaks align with the extract's high concentrations of flavonoids (0.267 mg/g) and total phenols (10.50 mg/g) as shown in table (1). These functional groups' existence indicates that phenolic and flavonoid chemicals were important for ZnO nanoparticle reduction, stability, and capping. Flavonoids and phenolic acids are examples of secondary metabolites originating from plants that exhibit characteristic signatures of C–O and aromatic C=C

vibrations, indicating their role in the creation of nanoparticles. However, *Q. infectoria*'s FTIR spectra revealed more functional groups, including peaks at 3433.25 cm^{-1} (O–H stretching), 2319.96 cm^{-1} (Zn–CO_2 bending), 1644.80 cm^{-1} (N–H bending or C=O stretching), and 1035.72 cm^{-1} (C=O stretching) (figure 4). Even though ZnO nanoparticles have a lower overall phenol (8.41 mg/g) and flavonoid (0.026 mg/g) content (Table 1), occurrence of further peaks might be related to the involvement of other phytochemicals or interaction of flavonoids, tannins and phenols.

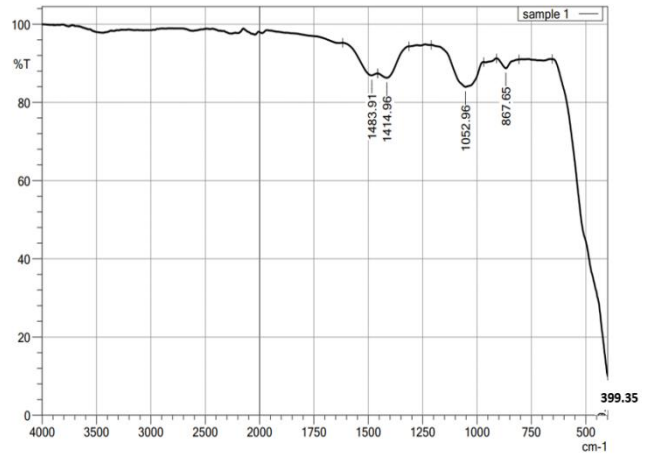

Fig. 3: FTIR spectrum of green-synthesized ZnO nanoparticles using *Q. brantii* leaf extract.

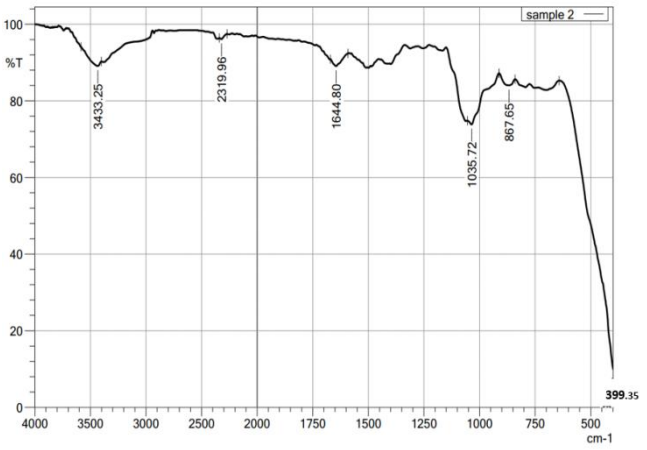

Fig. 4: FTIR spectrum of green-synthesized ZnO nanoparticles using *Q. infectoria* leaf extract.

The nano- scaled particles of the two species of oak exhibited wurtzite hexagonal structure, with a narrow diffraction peak which giving the approval of high crystallinity without impurities (Figures 5 and 6). The crystallite size was calculated via Debye–Scherrer equation valued as 27.55 nm for *Q. brantii* and 46.12 nm for *Q. infectoria*, suggesting that the higher phenolic and flavonoid content in *Q. brantii* promoted enhanced nucleation and more effective capping, thereby limiting crystal growth. In contrast, in *Q. infectoria* the capping efficiency was reduced due to lower flavonoid content that led to yield more extensive crystal growth. The results obtained were in parallel with previous reports that size of crystals often decreases as the phytochemical content increase in green extracts. For example, when *Aloe barbadensis Miller* aqueous leaf extract (2.45 an 0.45 mg/g fresh weight of phenols and flavonoids) used, ZnO NPs yielded crystallite diameter of 16.70 nm reported by [42]. As well as, [43] reported highly crystallinity nature with a hexagonal wurtzite structure of ZnO NP, with 12.2 nm diameter using Aloe vera extract. While, [44] demonstrated the well-defined formation of ZnO nanoparticles with pure wurtzite hexagonal crystals and an average diameter of 52 nm when miracle tree leaves were used, indicating their potential for efficient nanoparticle synthesis. [45] found that *Ocimum Tenuiflorum* zinc oxide crystalline size was 28.13 nm. [46] used Allium *Calocephalum Wendelbow* to obtained average crystallite size for Zinc Acetate 16.91 nm, 20.99 nm, and 21.25 nm, and for Zinc Chloride 28.19 nm, 20.99 nm. The crystallite size values obtained in the present study in parallel with previous reported sizes for green methods in synthesized ZnO NPs.

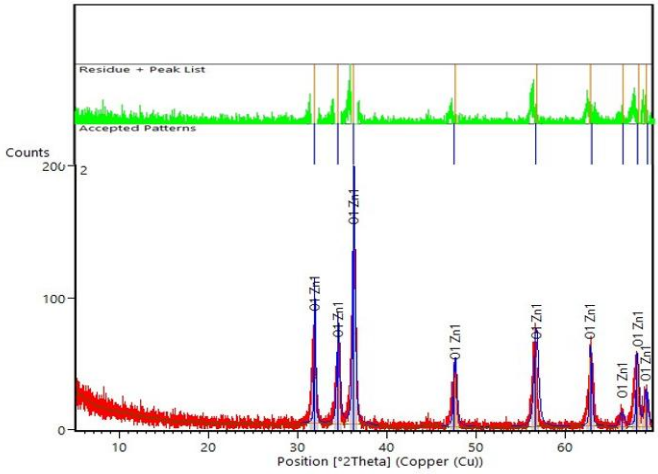

Fig. 5: X-ray Diffraction (XRD) for *Q. brantii* leaf extract

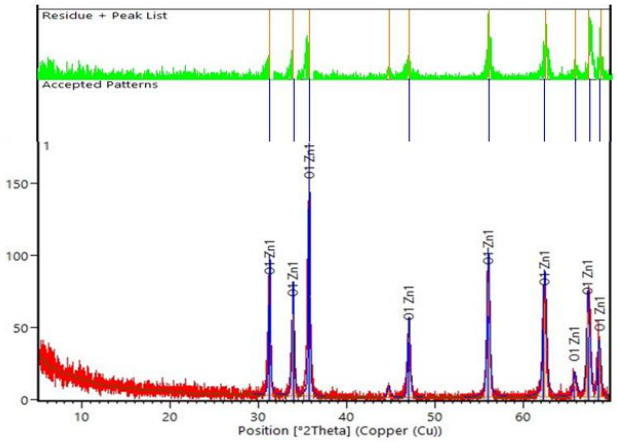

Fig. 6: X-ray Diffraction (XRD) for *Q. infectoria* leaf extract

The leaf extracts of *Quercus brantii* and *Quercus infectoria* mediated in ZnO NP synthesis a strong signal for zinc and oxygen were detected in EDX analysis, the presence of such strong peaks of both elements confirms the of ZnO NPs yield (Figures 7 and 8). For *Q. brantii*, the elemental composition was 86.98 wt.% Zn and 13.02 wt.% O. While for *Q. infectoria*, the composition was 84.28 wt.% Zn and 15.72 wt.% O (table 2). In both cases, Zn peaks appeared prominently at 1 and 8.6 keV, and oxygen (O) peaks with 0.50 keV for both species, which is consistent with reported EDX profiles of plant-mediated ZnO synthesis. [47] found

that ZnO nanoparticles synthesized using *Coriandrum sativum* leaf extract exhibited maximum absorbance at 333 nm and 348 nm for samples calcined at 100 °C and 550 °C, respectively, which corresponded to band gap energies of 3.56 eV and 3.72 eV, indicating a slight increase in band gap with higher calcination temperature. The results obtained related to element ratios are located within the typical ranges for Zn (35- 90 %) and O (10- 50 %). [48] used *Achillea wilhelmsii* for ZnO NP green synthesis, and the yield obtained was 36.80 % Zn and 51.3 % O. In addition, when *Arthrospira platensis* based for ZnO- synthesis, the yield was 56.60 and 20.4 % of Zn and O [49] While *Punica granatum* peel extract yielded 55.30 % Zn and 24.3 O % [50]. [39] obtained similar elemental ratio of Zn: O stoichiometry for ZnO NPs synthesis when they used Aloe vera. In conclusion the two oak species have been yielded stoichiometric elemental ratios, high grade pure ZnO nanoparticles and no impurities, that's in parallel with those reported in other related studies. The results of [51] revealed 75.12 and 23.55 % of Zn and O used *Plectranthus amboinicus* extract mediated in ZnO NP synthesis. Furthermore, [49] synthesized ZnO nanoparticles using *Pluchea indica*, with a composition of 20.5% oxygen, 29.3% carbon, and 50% zinc, indicating the successful incorporation of the expected elements in the nanoparticles. In another investigation, [52] confirmed similar ratios with high purity ZnO NPs when *Mucuna pruriens* (utilis) used. [53] confirmed that the mass percentages of Zn and O were 38.15 and 52.13% when they used *Limonium pruinosum* L. Chaz. leaf extract.

Table 2: the mass, normalized mass percent, and atom percent of elemental component (Zn and O) using *Q..brantii* and *Q. infctoria* leaf extracts

Q. brantii				
Element	***Mass (%)***	***Normalized mass (%)***	***Atom (%)***	***Error (%)***
Zinc	10.56	86.98	62.04	2.72
Oxygen	1.58	13.02	37.96	19.78
Total	12.14	100.00	100.00	
Q. infectoria				
Element	***Mass (%)***	***Normalized mass (%)***	***Atom (%)***	***Error (%)***
Zinc	10.19	84.28	56.74	2.73
Oxygen	1.90	15.72	43.26	18.53
Total	12.09	100.00	100.00	

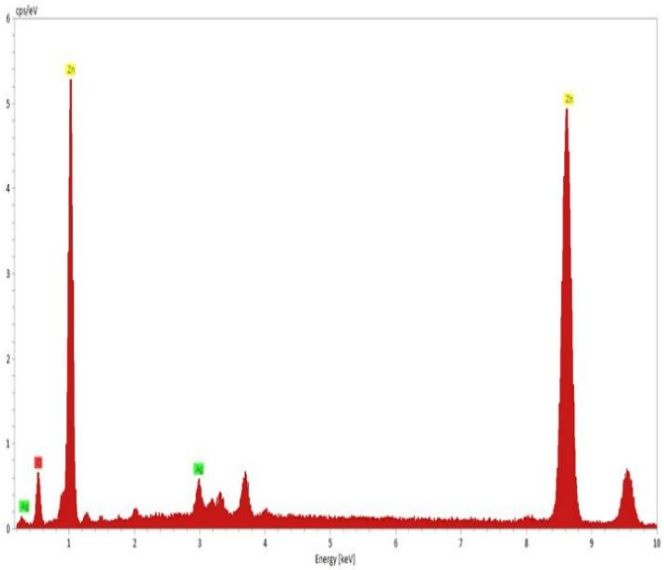

Fig. 7: EDX spectrum of synthesized ZnO NP from *Q. brantii* leaf extract

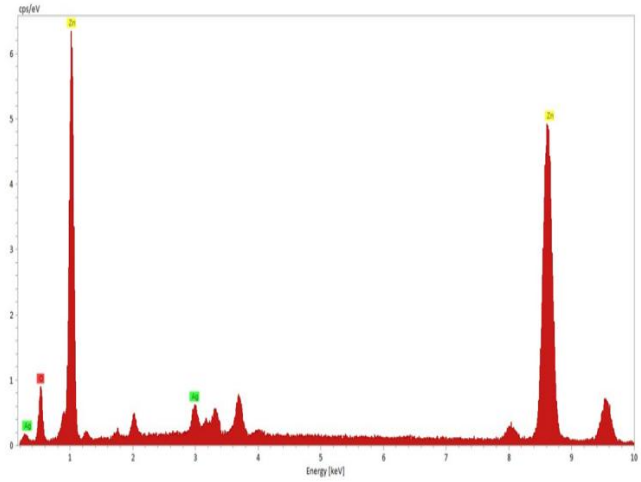

Fig. 8: EDX spectrum of synthesized ZnO NP from *Q. infectoria* leaf extract

After obtaining images of SEM for *Quercus brantii* and *Quercus infectoria* (Fig. 9), the images were processed using ImageJ software for measuring the circularity degree and particles diameter. The leaf extract of *Q. brantii* yielded NPs with a diameters range (46.64– 86.64 nm) with an average 46.11 nm (Fig.10). While, from *Q. infectoria* were averaged larger size nanoparticles 50.01 nm and more heterogenous range from 30.04 to 86.30 nm compared to Q. brantii (Fig. 11). Although the particle sizes of the two samples were similar, the phytochemicals in the leaf extracts likely played a role in stabilizing and capping the nanoparticles, which is reflected in the XRD peak intensities and crystallinity, rather than causing a significant difference in particle size. ZnO nanoparticles obtained from *Thymus vulgaris* extract averaged around 51–52 nm and were predominantly spherical [54-55] synthesized ZnO NPs from Aloe vera extract, the particles ranging from 30 to 42 nm. *Phoenix dactylifera* extract produced nanoparticles ranging from 18.1 to 61.6 nm with well-distributed spherical morphologies [56], and *Punica granatum* peel extract yielded particles of 10–45 nm in TEM/SEM images with a hydrodynamic diameter of ~62 nm, again showing largely spherical shapes [57]. The particles of both *Quercus* species characterized by their quasi-spherical and moderately irregular shapes, which is in parallel with the general characters of plant-mediated ZnO nanoparticle synthesis.

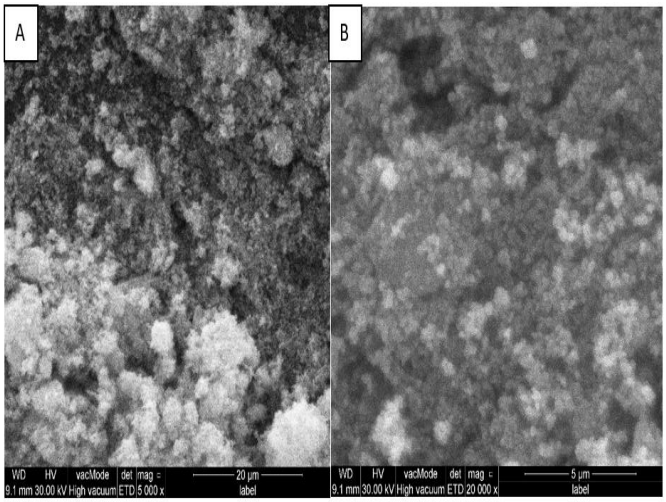

Fig. 9: Examples of SEM images of green ZnONPs. A: *Q. brantii* and B: *Q. infectoria*

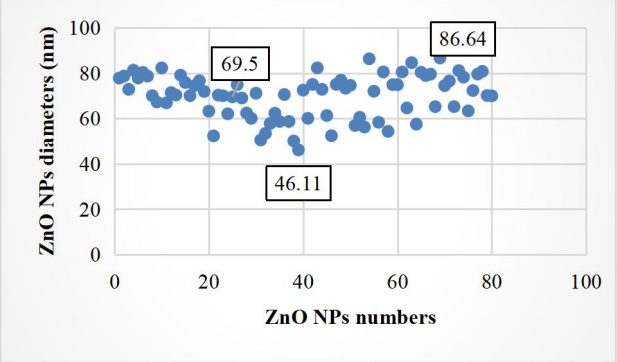

Fig.10 : The size distribution of ZnO NPs using *Q. brantii* leaves, showing mean, maximum, and minimum particle diameters (nm).

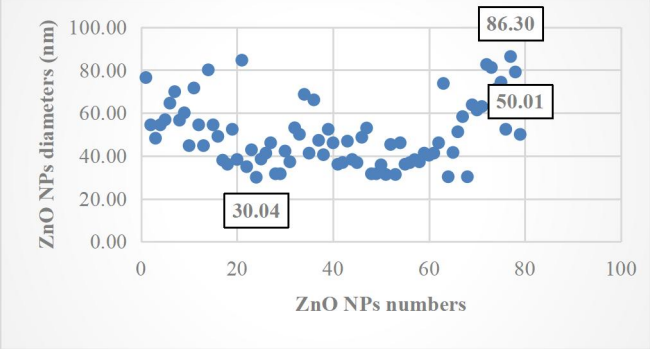

Fig.11: The size distribution of ZnO NPs using *Q. infectoria*, showing mean, maximum, and minimum particle diameters (nm).

Fig. 12: Circularity distribution of green synthesized ZnO NP using *Q. brantii* leaf extract, indicating shape uniformity and morphology.

Fig. 13: Circularity distribution of green synthesized ZnO NP using *Q. infectoria* leaf extract, indicating shape uniformity and morphology.

IV. CONCLUSION

Leaf extracts of *Q. brantii* and *Q. infectoria* demonstrated successful synthesis of ZnO NPs. The crucial determinants of size and morphology depend on the phytochemical content of the plant extract. The higher phenol and flavonoid content in *Q. brantii* leaves resulted in a smaller, and more homogenous particles. In contrast, *Q. infectoria*'s lower concentration for the two secondary metabolites resulted in a synthesis of larger and more heterogeneous particles. The results showed that oak species act as an effective green reductant and provide valuable manipulation of the natural phytochemical composition for optimizing the synthesized nanomaterials characterization.

ACKNOWLEDGMENT

The authors gratefully acknowledge Salahaddin University–Erbil for providing the facilities and academic support necessary to conduct this research. This study was carried out as part of the requirements for the Master of Science (M.Sc.) degree at Salahaddin University–Erbil.

CONFLICT OF INTEREST

The authors have no competing interests.

CONFLICT OF INTEREST

The authors declare that they have no conflict of interest.

REFERENCES

[1] H. Bokhari, "Exploitation of microbial forensics and nanotechnology for the monitoring of emerging pathogens," *Critical Reviews in Microbiology,* vol. 44, no. 4, pp. 504-521, 2018. https://doi.org/10.1080/1040841X.2018.1444013

[2] X.-Q. Zhou *et al.*, "Zinc oxide nanoparticles: synthesis, characterization, modification, and applications in food and agriculture," *Processes,* vol. 11, no. 4, p. 1193, 2023. https://doi.org/10.3390/pr11041193

[3] S. A. Qadir, C. N. Fathulla, and S. A. Amin, "Influence of Zinc Oxide Nano Spray on the Growth and Development of Bryophyllum pinnatum," *Polytechnic Journal,* vol. 13, no. 1, p. 23, 2024.https://doi.org/10.59341/2707-7799.1836

[4] I. Khan, K. Saeed, and I. Khan, "Nanoparticles: Properties, applications and toxicities," *Arabian journal of chemistry,* vol. 12, no. 7, pp. 908-931, 2019. https://doi.org/10.1016/j.arabjc.2017.05.011

[5] J. W. Rasmussen, E. Martinez, P. Louka, and D. G. Wingett, "Zinc oxide nanoparticles for selective destruction of tumor cells and potential for drug delivery applications," *Expert opinion on drug delivery,* vol. 7, no. 9, pp. 1063-1077, 2010. https://doi.org/10.1517/17425247.2010.502560.

[6] A. Sirelkhatim *et al.*, "Review on zinc oxide nanoparticles: antibacterial activity and toxicity mechanism," *Nano-micro letters,* vol. 7, no. 3, pp. 219-242, 2015. https://doi.org/10.1007/s40820-015-0040-x

[7] K. Sachin and S. K. Karn, "Microbial fabricated nanosystems: Applications in drug delivery and targeting," *Frontiers in Chemistry,* vol. 9, p. 617353, 2021. https://doi.org/10.3389/fchem.2021.617353

[8] S. Iravani, "Green synthesis of metal nanoparticles using plants," *Green chemistry,* vol. 13, no. 10, pp. 2638-2650, 2011. https://doi.org/10.1039/C1GC15386B

[9] P. Aarthye and M. Sureshkumar, "Green synthesis of nanomaterials: An overview," *Materials Today: Proceedings,* vol. 47, pp. 907-913, 2021. https://doi.org/10.1016/j.matpr.2021.04.564

[10] M. Ramzan *et al.*, "Synergistic effect of zinc oxide nanoparticles and Moringa oleifera leaf extract alleviates cadmium toxicity in Linum usitatissimum: Antioxidants and physiochemical studies," *Frontiers in plant science,* vol. 13, p. 900347, 2022.

[11] M. Stan, A. Popa, D. Toloman, T.-D. Silipas, and D. C. Vodnar, "Antibacterial and antioxidant activities of ZnO nanoparticles synthesized using extracts of Allium sativum, Rosmarinus officinalis and Ocimum basilicum," *Acta Metallurgica Sinica (English Letters),* vol. 29, no. 3, pp. 228-236, 2016.

[12] F. A. Gutiérrez-Miceli, M. Á. Oliva-Llaven, M. C. Luján-Hidalgo, M. C. Velázquez-Gamboa, D. González-Mendoza, and Y. Sánchez-Roque, "Zinc oxide phytonanoparticles' effects on yield and mineral contents in fruits of tomato (Solanum lycopersicum L. cv. Cherry) under field conditions," *The Scientific World Journal,* vol. 2021, no. 1, p. 5561930, 2021.

[13] Z. A. Mahmoud, M. A. Atiya, and A. K. Hassan, "The Influence of Support Materials on The Photo-Fenton-like Degradation of Azo Dye Using Continuous Nanoparticles Fixed-bed Column," *Al-Khwarizmi Engineering Journal,* vol. 18, no. 4, pp. 14-31, 2022.

[14] A. I. Osman *et al.*, "Synthesis of green nanoparticles for energy, biomedical, environmental, agricultural, and food applications: A review," *Environmental Chemistry Letters,* vol. 22, no. 2, pp. 841-887, 2024. https://doi.org/10.1007/s10311-023-01682-3

[15] N. Rani, P. Singh, S. Kumar, P. Kumar, V. Bhankar, and K. Kumar, "Plant-mediated synthesis of nanoparticles and their applications: A review," *Materials Research Bulletin,* vol. 163, p. 112233, 2023. https://doi.org/10.1016/j.materresbull.2023.112233

[16] M. C. Ogwu, S. C. Izah, and M. T. Joshua, "Ecological and environmental determinants of phytochemical variability in forest trees," *Phytochemistry Reviews,* pp. 1-29, 2025. https://doi.org/10.1007/s11101-025-10066-0

[17] E. Coyotl-Martinez, J. A. Hernández-Rivera, J. L. A. Parra-Suarez, S. R. Reyes-Carmona, and A. Carrasco-Carballo, "Phytochemical Profile, Antioxidant and Antimicrobial Activity of Two Species of Oak: *Quercus* Sartorii and *Quercus* Rysophylla," *Applied Biosciences,* vol. 4, no. 1, p. 13, 2025. https://doi.org/10.3390/applbiosci4010013

[18] A. A. Ahmed, N. A.-R. Tahir, and S. A. Qadir, "Nutrient Dynamics in Oak Forests of Iraqi Kurdistan due to Altitudinal and Geospatial Influences," *Passer Journal of Basic and Applied Sciences,* vol. 7, no. 1, pp. 114-120, 2025. https://doi.org/10.24271/PSR.2025.415060.1387

[19] N. R. Khwarahm, "Mapping current and potential future distributions of the oak tree (*Quercus* aegilops) in the Kurdistan Region, Iraq," *Ecological Processes,* vol. 9, no. 1, pp. 1-16, 2020. https://doi.org/10.1186/s13717-020-00259-0.

[20] M. Nasser, "Forests and forestry in Iraq: prospects and limitations," *The Commonwealth Forestry Review,* pp. 299-304, 1984. https://www.jstor.org/stable/42606437

[21] A. K. Srivastava, P. Mishra, and A. K. Mishra, "Effect of climate change on plant secondary metabolism: An ecological perspective," in *Evolutionary diversity as a source for anticancer molecules*: Elsevier, 2021, pp. 47-76. https://doi.org/10.1016/B978-0-12-821710-8.00003-5

[22] W. Sun and M. H. Shahrajabian, "Therapeutic potential of phenolic compounds in medicinal plants—Natural health products for human health," *Molecules,* vol. 28, no. 4, p. 1845, 2023. https://doi.org/10.3390/molecules28041845

[23] J. Rahman and D. Jaff, "Variation in phytochemical, physiochemical contents and toxicity of Prangos platychlaena Boiss in Halgurd mountain of Iraqi Kurdistan," *Iraqi Journal of Agricultural Sciences,* vol. 51, no. 1, 2020. https://doi.org/10.36103/ijas.v51i1.943

[24] K. L. Singh and G. Bag, "Phytochemical analysis and determination of total phenolics content in water extracts of three species of Hedychium," *Int J PharmTech Res,* vol. 5, no. 4, pp. 1516-21, 2013. https:///doi/full/10.5555/20143020385

[25] M. F. Ahad *et al.*, "Comparative pharmacological potential of Ceriops decandra (Griff.) and Ceriops tagal Linn: medicinal plants of the Sundarbans," *Journal of Medicinal Plants,* vol. 9, no. 4, pp. 14-23, 2021. https://doi.org/10.22271/plants.2021.v9.i4a.1306

[26] Z. Song *et al.*, "Characterization of optical properties of ZnO nanoparticles for quantitative imaging of transdermal transport," *Biomedical optics express,* vol. 2, no. 12, pp. 3321-3333, 2011. https://doi.org/10.1364/BOE.2.003321

[27] H. P. Klug and L. E. Alexander, *X-ray diffraction procedures: for polycrystalline and amorphous materials*. 1974.https://ui.adsabs.harvard.edu/abs/1974xdpf.book.....K/abstract

[28] H. A. Al LEHAIBI, "Control of zinc corrosion in acidic media: Green fenugreek inhibitor," *Transactions of Nonferrous Metals Society of China,* vol. 26, no. 11, pp. 3034-3045, 2016. https://doi.org/10.1016/S1003-6326(16)64434-5

[29] Z. L. Wang, "Zinc oxide nanostructures: growth, properties and applications," *Journal of physics: condensed matter,* vol. 16, no. 25, p. R829, 2004. https://doi.org/10.1088/0953-8984/16/25/R01

[30] F. Shakuri, G. Eghlima, H. Behboudi, and M. Babashpour-Asl, "Phytochemical variation, phenolic compounds and antioxidant activity of wild populations of Iranian oak," *Scientific Reports,* vol. 15, no. 1, p. 6534, 2025.https://doi.org/10.1038/s41598-025-90991-4

[31] A. M. Hashim, B. M. Alharbi, A. M. Abdulmajeed, A. Elkelish, W. N. Hozzein, and H. M. Hassan, "Oxidative stress responses of some endemic plants to high altitudes by intensifying antioxidants and secondary metabolites content," *Plants,* vol. 9, no. 7, p. 869, 2020. https://doi.org/10.3390/plants9070869

[32] L. Pan *et al.*, "Altitudinal variation on metabolites, elements, and antioxidant activities of medicinal plant asarum," *Metabolites,* vol. 13, no. 12, p. 1193, 2023. https://doi.org/10.3390/metabo13121193

[33] A. Golob, N. Luzar, I. Kreft, and M. Germ, "Adaptative responses of common and tartary buckwheat to different altitudes," *Plants,* vol. 11, no. 11, p. 1439, 2022.https://doi.org/10.3390/plants11111439

[34] J. Krajczewski, R. Ambroziak, and A. Kudelski, "Substrates for surface-enhanced Raman scattering formed on nanostructured non-metallic materials: preparation and characterization," *Nanomaterials,* vol. 11, no. 1, p. 75, 2020. https://doi.org/10.1039/C7RA01034F

[35] G. J. Nanomed, "Use of honey in stabilization of ZnO nanoparticles synthesized via hydrothermal route and assessment of their antibacterial activity and cytotoxicity. Glob," *J. Nanomed,* vol. 2, pp. 37-41, 2017.http://dx.doi.org/10.19080/GJN.2017.02.555585

[36] R. S. Mohammed, A. Sudhakaran, M. Y. A. Mostafa, and G. Abbady, "Synthesize of ZnO and CuO nanoparticles with plasma jet at different treatment times and testing its optical parameters with UV-Vis-NIR," *Applied Physics A,* vol. 130, no. 8, p. 533, 2024. https://doi.org/10.1007/s00339-024-07651-z

[37] S. Singh, J. V. Gade, D. K. Verma, B. Elyor, and B. Jain, "Exploring ZnO nanoparticles: UV–visible analysis and different size estimation methods," *Optical Materials,* vol. 152,p.115422,2024. https://doi.org/10.1016/j.optmat.2024.115422

[38] C. Mahajan, "Structural, Surface Wettability, Optical, Urbach Tail, and Electrical Properties of Spray Pyrolyzed ZnO Thin Films: Role of Air Flow Rate: CM Mahajan," *JOM,* vol. 75, no. 2, pp. 448-458, 2023. https://doi.org/10.1007/s11837-022-05621-5

[39] C. Klingshirn, "ZnO: material, physics and applications," *ChemPhysChem,* vol. 8, no. 6, pp. 782-803, 2007.https://doi.org/10.1002/cphc.200700002

[40] K. Elumalai, S. Velmurugan, S. Ravi, V. Kathiravan, and S. Ashokkumar, "RETRACTED: Green synthesis of zinc oxide nanoparticles using Moringa oleifera leaf extract and evaluation of its antimicrobial activity," ed: Elsevier, 2015.https://doi.org/10.1016/j.saa.2015.02.011

[41] A. K. Arora, S. Devi, V. S. Jaswal, J. Singh, M. Kinger, and V. D. Gupta, "Synthesis and characterization of ZnO nanoparticles," *Orient. J. Chem,* vol. 30, no. 4, pp. 1671-1679, 2014. http://dx.doi.org/10.13005/ojc/300427

[42] M. Abu-Gharbia, J. Salem, and G. Al-Arabi, "Biosynthesis of zinc oxide nanoparticles using Aloe vera leaves extract and their antibacterial impact," *Bulletin of Pharmaceutical Sciences Assiut University,* vol. 47, no. 1, pp. 499-517, 2024.https://doi.org/10.21608/bfsa.2023.239425.1934

[43] S. Shrestha *et al.*, "Exploring Photocatalytic, Antimicrobial and Antioxidant Efficacy of Green-Synthesized Zinc Oxide Nanoparticles," *Nanomaterials,* vol. 15, no. 11, p. 858, 2025. https://doi.org/10.3390/nano15110858

[44] I. Ngom, N. Ndiaye, A. Fall, M. Bakayoko, B. Ngom, and M. Maaza, "On the use of Moringa oleifera leaves extract for the biosynthesis of NiO and ZnO nanoparticles," *MRS Advances,* vol. 5, no. 21-22, pp. 1145-1155, 2020. https://doi.org/10.1557/adv.2020.212.

[45] E. A. Dwidar and F. Fouda, "Synthesis and characterization of zinc oxide nanoparticles (ZnO-NPs) from leaves of some plants," *Annals of Agricultural Science, Moshtohor,* vol. 61, no. 1, pp. 97-110, 2023. https://dx.doi.org/10.21608/assjm.2023.190585.1204

[46] A. N. Abdulqudos and A. F. F. Abdulrahman, "Biosynthesis and characterization of ZnO nanoparticles by using leaf extractionof allium calocephalum wendelbow plant," *Passer Journal of Basic and Applied Sciences,* vol. 4, no.2,pp.113-126,2022. https://doi.org/10.24271/psr.2022.343112.1136

[47] G. Yashni, A. Al-Gheethi, R. Mohamed, and M. A. Hashim, "Green synthesis of ZnO nanoparticles by Coriandrum sativum leaf extract: structural and optical properties," *Desalination and Water Treatment,* vol. 167, pp. 245-257, 2019. https://doi.org/10.5004/dwt.2019.24584

[48] M. Gulnar *et al.*, "Green Synthesis of Zinc Oxide Nanoparticles Using Achillea Wilhelmsii Extract: A Biological Approach," *Journal of Nanostructures,* vol. 13, no. 3, pp. 685-692, 2023. https://doi.org/10.22052/JNS.2023.03.009

[49] E. F. El-Belely *et al.*, "Green synthesis of zinc oxide nanoparticles (ZnO-NPs) using Arthrospira platensis (Class: Cyanophyceae) and evaluation of their biomedical activities," *Nanomaterials,* vol. 11, no. 1, p. 95, 2021. https://doi.org/10.3390/nano11010095

[50] U. L. Ifeanyichukwu, O. E. Fayemi, and C. N. Ateba, "Green synthesis of zinc oxide nanoparticles from pomegranate (Punica granatum) extracts and characterization of their antibacterial activity," *Molecules,* vol. 25, no. 19, p. 4521, 2020. https://doi.org/10.3390/molecules25194521

[51] S. Vijayakumar, B. Vaseeharan, B. Malaikozhundan, and M. Shobiya, "Laurus nobilis leaf extract mediated green synthesis of ZnO nanoparticles: Characterization and biomedical applications," *Biomedicine & Pharmacotherapy,* vol. 84, pp. 1213-1222, 2016. https://doi.org/10.1016/j.biopha.2016.10.038

[52] N. P. Gamedze, D. M. Mthiyane, S. Mavengahama, M. Singh, and D. C. Onwudiwe, "Biosynthesis of ZnO nanoparticles using the aqueous extract of Mucuna pruriens (utilis): structural characterization, and the anticancer and antioxidant activities," *Chemistry Africa,* vol. 7, no. 1, pp. 219-228, 2024.https://doi.org/10.1007/s42250-023-00750-z

[53] B. Naiel, M. Fawzy, M. W. A. Halmy, and A. E. D. Mahmoud, "Green synthesis of zinc oxide nanoparticles using Sea Lavender (Limonium pruinosum L. Chaz.) extract: characterization, evaluation of anti-skin cancer, antimicrobial and antioxidant potentials," *Scientific Reports,* vol. 12, no. 1, p. 20370, 2022.https://doi.org/10.1038/s41598-022-24805-2

[54] S. T. Karam and A. F. Abdulrahman, "Green synthesis and characterization of ZnO nanoparticles by using thyme plant leaf extract," in *Photonics*, 2022, vol. 9, no. 8, p. 594: MDPI. https://doi.org/10.3390/photonics9080594

[55] L. Tabassam, M. J. Khan, S. Hussain, S. A. Khattak, S. K. Shah, and A. S. Bhatti, "Structural, optical and antimicrobial characteristics of ZnO green nanoparticles," *Journal of Sol-Gel Science and Technology,* vol. 101, no. 2, pp.401-410,2022.https://doi.org/10.1007/s10971-022-05726-y.

[56] J. A. A. Abdullah, M. J. Rosado, A. Guerrero, and A. Romero, "Eco-friendly synthesis of ZnO-nanoparticles using Phoenix dactylifera L., polyphenols: physicochemical, microstructural, and functional assessment," *New Journal of Chemistry,* vol. 47, no. 9, pp. 4409-4417, 2023.https://doi.org/10.21203/rs.3.rs-1934475/v2

[57] A. Fouda *et al.*, "Green synthesis of zinc oxide nanoparticles using an aqueous extract of punica granatum for antimicrobial and catalytic activity," *Journal of Functional Biomaterials,* vol. 14, no. 4, p. 205, 2023. https://doi.org/10.3390/jfb14040205